Study of polarization-dependent energy coupling between near-field optical probe and mesoscopic metal structure

A. Gademann and I. V. Shvets[a)]
SFI Laboratory, Physics Department, Trinity College, Dublin 2, Ireland

C. Durkan
Department of Engineering, University of Cambridge, Trumpington Street, Cambridge CB2 1PZ, United Kingdom

(Received 31 January 2003; accepted 4 January 2004)

We present an experimental study of the coupling of light from a probe of a scanning near-field optical microscope (SNOM) into a mesoscopic structure consisting of gold stripes with varying separations. We demonstrate that the coupling efficiency depends upon the polarization direction in the probe relative to the stripes as well as the separation between the lines. Two possible explanations for a contrast reversal effect in between *s*- and *p*-polarized light are given. One is based on the excitation of a quasi-transverse electric and magnetic mode in the mesoscopic transmission line. For this explanation we have made a prediction of the condition of the maximum coupling efficiency through the approach of impedance matching. The second explanation is based on surface plasmon excitation in the gold structure. The present results can also be of importance in the development of new concepts of probes for SNOM. © *2004 American Institute of Physics.*
[DOI: 10.1063/1.1649453]

I. INTRODUCTION

The study of electromagnetic coupling into small metal structures is motivated by fundamental research and also by possible applications of the optical properties of such structures. In the case of coupling of light from a probe of a scanning near-field optical microscope (SNOM) into a metal structure there is additional interest driven by the issues of understanding the mechanisms of the contrast formation, contrast polarization dependency, and also by the interest of developing more efficient SNOM probes. In the case of certain metals like gold and silver showing significant plasmon resonance efficiency, there is a further issue of understanding the contribution of plasmons into the optical properties of the structure. For example, squeezing of the optical near-field due to plasmon coupling was observed above a chain of Au particles.[1] The preset experimental study aims at achieving improved understanding of the coupling of light from a fiber probe of a scanning near-field optical microscope to a mesoscopic metal structure. In particular, we focus on the issues of the dependency of coupling on the polarization of light at the output of the probe and the size of the structure.

The metal structure consisting of parallel metal lines deposited on a dielectric substrate is a convenient model structure due to its simplicity and also due to expected significant dependency of the optical properties of the light polarization. Optical response of periodic arrays of metal and dielectric lines has been modeled theoretically.[2] Strong polarization dependency of optical properties of Au nanowire grating in the far field was observed by Schider *et al.*[3]

We performed the experiment using scanning near-field optical microscopy (SNOM),[4] a technique which allows resolution well below the diffraction limit. The key element of the technique is a probe, usually consisting of a tapered optical fiber coated with metal to form an aperture of the size 30–150 nm at the end. The probe forms a localized light source, illuminating only the part of the sample close to the aperture. When using polarized light it is therefore possible to study the effect of the light on the sample and sample structure, depending on the polarization direction, close to the aperture. This was shown using magnetic samples with magneto optical Kerr effect.[5]

It is well appreciated that more commonplace acceptance of SNOM as a measurement technique depends on development of new probes capable of better resolution and more straightforward image interpretation. The work on new SNOM probes has received much attention from the near-field optics community.[6,7]

II. EXPERIMENT

The instrument used for the experiment is a reflection-mode SNOM. The collection of the light is performed by an elliptical mirror.[8–10] The probe/sample interface is located at the first focal point, while the light is collected by a photomultiplier tube (PMT) located at the second focal point. The optical layout can be seen in Fig. 1.

The probes are produced by tube etching proposed by Stockle *et al.*[11] They are coated to have ~40-nm-thick aluminum film at the tip apex forming an aperture at the very end of the tip. The laser used is a 635 nm diode laser. The light coming from the tip can be polarized by using a quarter wave plate and a half wave plate. The polarization is mea-

[a)]Author to whom correspondence should be addressed; electronic mail: ivchvets@tcd.ie

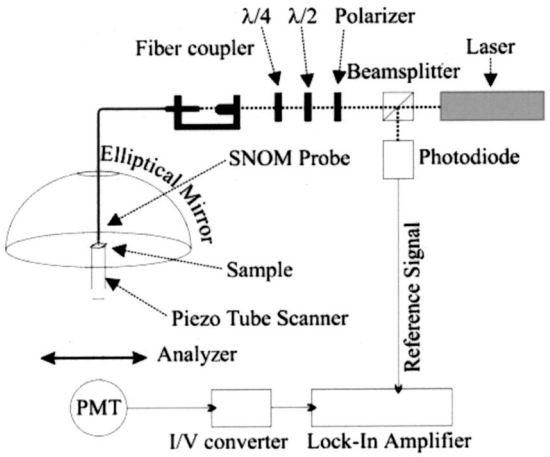

FIG. 1. Schematics of the optical layout of the reflection mode SNOM.

sured by placing an analyzer in between the probe and the PMT and it could be chosen in the range of 1:1–1:20 with alignment along any desired direction.

Two types of samples were produced by e-beam lithography. They consisted of gold lines, 20 nm thick and 1000 nm wide, formed on a silicon substrate. The distance between the lines is 250 nm for sample 1 and varies regularly between 200 and 1000 nm for sample 2. The area between the lines is the bare silicon substrate.

Due to the high confinement of light in the aperture region of the probe, a distance feedback mechanism is required to maintain the sample within the near field of the aperture. The technique used here was shear-force detection,[12,13] which allows us to simultaneously (1) image the sample topography and (2) obtain SNOM images. The probe could be kept at a constant height of 5–30 nm above the sample, with the accuracy of ± 2 nm using the shear-force feedback system described in Ref. 14.

III. RESULTS

Figure 2 shows two optical SNOM images of a 4 μm$\times$4 μm area of sample 1. Figure 2(a) is recorded with light polarized parallel to the Au lines (TM polarization) and Fig. 2(b) with light polarized perpendicular to the lines (TE polarization). An analyzer was not used in these experiments.

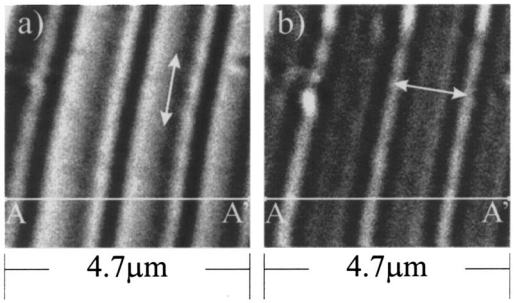

FIG. 2. Scans of the same area of the sample taken with polarization along the transmission line structures (TM polarization) (a) and perpendicular to them (TE polarization) (b). Arrows indicate the polarization directions used for the respective images.

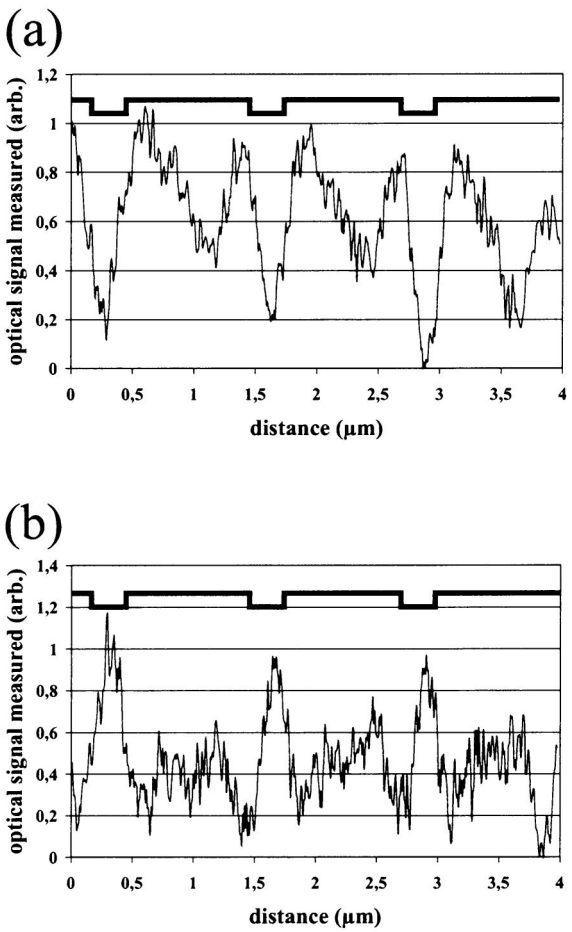

FIG. 3. Representative cross sections taken at the lines AA′ marked in Figs. (2a) and (2b). Thin lines of Figs. (3a) and (3b) represent the optical intensity signals for TM and TE polarizations, respectively. The thick lines represent topography of the structure as position reference.

Particles of dust identifiable on both images indicated that they were taken at the same area of the sample. Figure 2(a) shows the line as bright and the gap as dark, while Fig. 2(b) shows the line as dark and the gap as bright. When only material reflectivity is used to interpret the images, Fig. 2(a) can be explained, taking into account that the reflectivity of gold is higher compared to silicon. But Fig. 2(b) could not be explained. When comparing the actual measured intensities, taken as an average on top of the Au lines, it shows that the intensity change in between the two polarization directions is approximately 10%. Whereas if the mean values measured in between the lines are taken, a change of polarization results in an intensity change of up to 70%. This can be seen in the profiles (Fig. 3) taken at the representative cross-section AA′ of Fig. 2.

For details of interpretation of the results presented in Figs. 2 and 3 we refer the reader to our earlier publications.[8,10] These publications deal with the contrast formation in a reflection-mode SNOM and dependency of the contrast on the polarization of light. The test samples employed in the studies[8,10] are rather similar to the ones used in this study: metal stripes deposited on a dielectric substrate. There were two substantial differences. First, in Refs. 8 and 10, unlike in some of the samples used in the present study,

separation between the lines was constant. Second, the metal stripes in the present study are lines of Au while in Refs. 8 and 10 they were lines of Cr. In this article we will focus on the consequences stemming from these differences. However, we first apply the main conclusions drawn in Refs. 8 and 10 related to the obvious similarities between the results presented here and the earlier publications regarding the polarization dependence of the optical SNOM contrast. For example, for longitudinal polarization [Fig. 2(a)], Au lines are bright and the Si substrate between the lines is dark. This is due to greater reflectivity of Au than that of Si and also due to shadowing of light coming from the probe when it is placed in between the Au lines. When the polarization is rotated and made perpendicular to the lines [Fig. 2(b)], the contrast is reversed. The contrast reversal takes place due to the increase in measured intensity from the areas in between the Au lines. The contrast reversal is due to more efficient coupling of light with such a perpendicular polarization from the probe to the structure. In the case of perpendicular polarization, a transverse electric and magnetic (TEM) mode is launched when the probe is placed in between the Au lines, whereas it cannot be launched in the case of longitudinal polarization. Fully in line with conclusion of Refs. 8 and 10 we now observe that the signal intensity above the metal lines is mainly not polarization sensitive, but the one above the Si substrate in between the lines is.

Two possible explanations could be taken into account here. The first explanation models each pair of the nearest gold stripes as a transmission line. Such a transmission line can support TE mode with the polarization directed perpendicular to the lines. On the contrary, for the TM polarization the transmission line cannot support the mode. As a result the light cannot be efficiently coupled into the structure and therefore it is reflected back into the SNOM probe.

The second explanation is based on the local excitation of surface plasmons in the gold surface. The plasmon propagation direction is dependent on the polarization of the exciting light. Results of the letter in Ref. 15 suggest that generally plasmons propagate along the probe polarization direction. When the surface plasmon propagates to an edge boundary of a gold stripe it can scatter and reemit light which can then be detected with the PMT. As a result, an image taken with TE polarized light should show enhanced light detected at the edges next to the gaps.

Figure 4 shows topography and the optical SNOM images of a 9.3 μm$\times$9.3 μm area of the second sample. Figure 4(a) is the shear-force image of the sample and Figs. 4(b) and 4(c) are the optical images with the main axis of polarization parallel and perpendicular to the lines, respectively. The same dust particles identifiable on all three images indicate that the scans are all taken at the same area. The tip used for this experiment had an approximate aperture of 150 nm, as confirmed by scanning electron microscope for probes produced in the same way. An analyzer was not used in this experiment. Optical results presented in Figs. 2 and 4 with the same direction of polarization compare well. Once the polarization direction is set perpendicular to the lines (TE polarization) an increase in signal intensity in the gaps between the gold lines is observed compared to the images

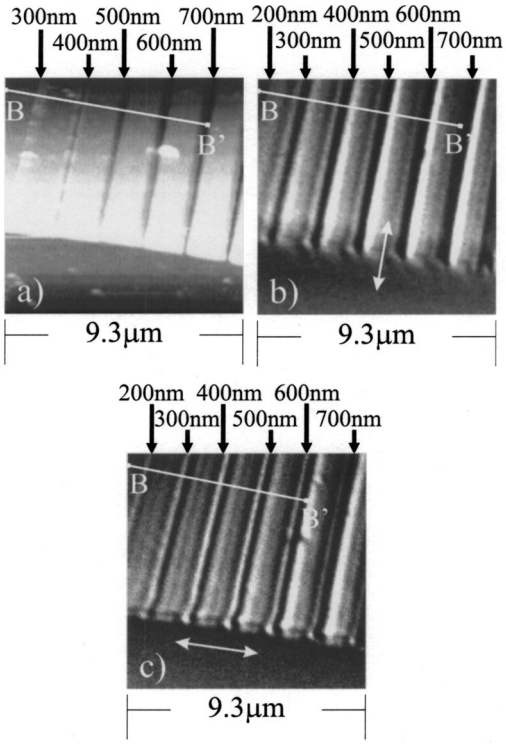

FIG. 4. Scans of the same area of the sample 2. (a) Shear-force topography image, (b) and (c) optical images taken with light polarized along the stripes and perpendicular to them, respectively. The polarization direction used for the respective image is indicated in the two optical images by arrows.

measured with parallel polarized light (TM polarization). Figure 5 shows this in the representative cross section. However, there is an additional feature in the result shown in Fig. 4. As the gap gets wider from 200 to 400 nm, the intensity of the optical signal measured at the gap intensity increases and then with, further increase in the gap width, it decreases provided the polarization is TE. The maximum/minimum combination visible on the right hand side of the gap and the left hand side of the lines in both optical images of Fig. 4 is most likely due to shadowing effects and a not totally symmetric collection of the light. Due to the fact that this minimum/maximum combination is independent of the polarization direction it does not contribute to the effect described here. Similar observation was made by us in Refs. 8, 10, and 16.

Figure 6 shows topography and optical SNOM images of a 9.3 μm$\times$9.3 μm area of the second sample. Figure 6(a) shows the shear-force image of the sample and Fig. 6(b) shows the optical image taken with polarization perpendicular to the gold lines (TE). The same dust particles identifiable on both images indicate that the scans are taken at the same area, and they can also be identified in the images of Fig. 4 showing the relation between the images. The tip used for these scans had an aperture larger than the one used for the previous scans. It was in the range of 180–200 nm. Comparing Figs. 4(c) and 6(b) shows the same general characteristics of a higher intensity in the gaps and a change of intensity depending on gap width provided that TE polarization was used. In Fig. 6(b) though the maximum intensity is observed when the gap width is 600 nm compared to 400 nm in Fig. 4(c). This is shown by the line cross-section (see Fig. 7).

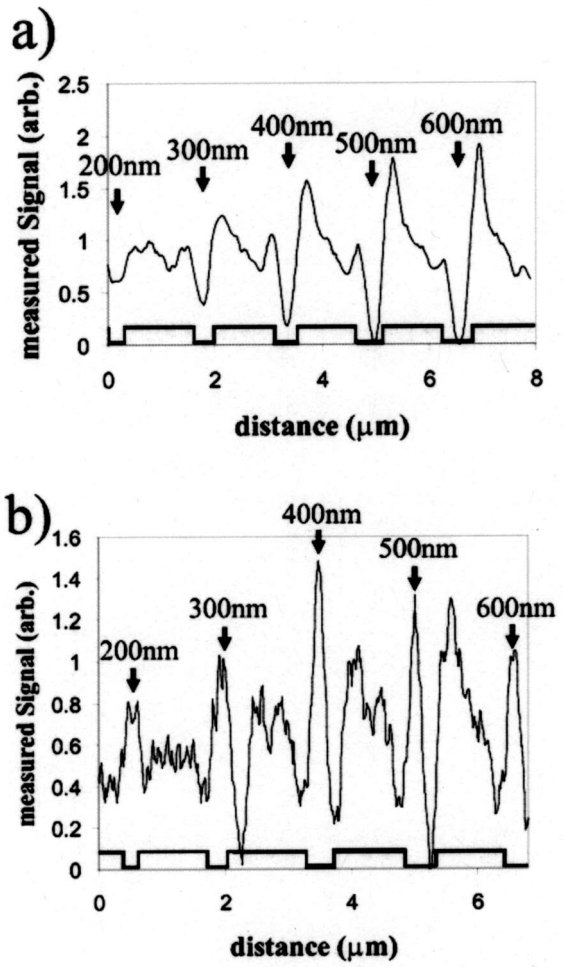

FIG. 5. Representative cross section taken at the lines BB′ marked in Fig. 4 for TM polarization [5(a)] and TE polarization [5(b)]. The thin lines of Figs. 5(a) and 5(b) represent optical intensity signals for TM and TE polarizations, respectively. The thick lines represent topography of the structure as position reference.

IV. DISCUSSION

In our view the results could be explained using two different approaches. The first one is based on microwave theory. In microwave theory, a clear distinction is made between transmission lines and waveguides.[17] Transmission lines consist of two or more conductors separated by a dielectric. They are able to support transverse electric and magnetic (TEM) modes or quasi-TEM modes, without any cutoff frequency. Waveguides are generally represented by a metal tube of circular, rectangular, or other cross section filled with a dielectric. They cannot support a true TEM mode, in which both field vectors E and H are perpendicular to the propagation direction. Instead they support TE_{mn} (transverse electric) or TM_{mn} (transverse magnetic) modes with only electric or magnetic field vector perpendicular to the waveguide axis, respectively. Each mode of a waveguide is characterized by its cutoff frequency.

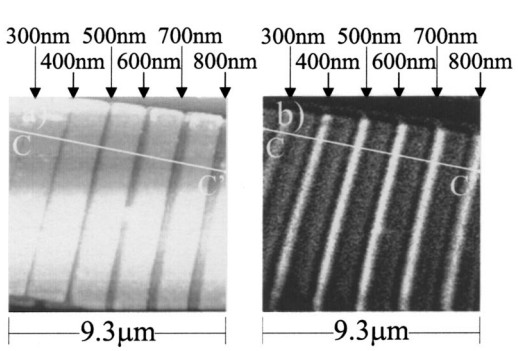

FIG. 6. Scans of the same area of sample 2. (a) Shear-force topography image and (b) an optical image taken with light polarized perpendicular to the stripes.

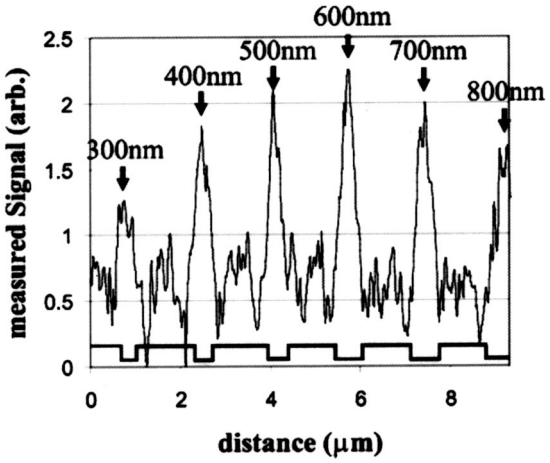

FIG. 7. Representative cross sections taken at the lines CC′ marked in Fig. 6. The thin line represents optical intensity signal for TE light polarization. The thick line represents topography of the structure as position reference.

The efficiency of electromagnetic coupling from waveguides to transmission lines depends upon the polarization direction in the waveguide with respect to the transmission line axis,[18] and on the characteristic impedances of both structures. The concept of impedance matching is commonly used in the radio- and microwave frequency range. In the optical frequency range impedance matching is much more difficult to demonstrate due to the submicron size and the difficulties with fabricating the optical structures required for such experiments. The notion of optical impedance is rarely used.

It should be noted that each pair of Au lines forms a coplanar transmission line. It can be modeled as a coplanar strip transmission line [Fig. 8(a)] or a coplanar waveguide [Fig. 8(b)]. To get an approximate idea of the impedance, value formulas from microwave textbooks were used, which should give an indication of the values. The analytical expression for the impedance Z_0[19] for the coplanar stripline is

$$Z_0 = \frac{120 \cdot \pi}{\sqrt{\epsilon_e}} \frac{K(k)}{K(k')}. \tag{1}$$

Impedance of the coplanar waveguide is

$$Z_0 = \frac{30 \cdot \pi}{\sqrt{\epsilon_e}} \frac{K(k')}{K(k)}. \tag{2}$$

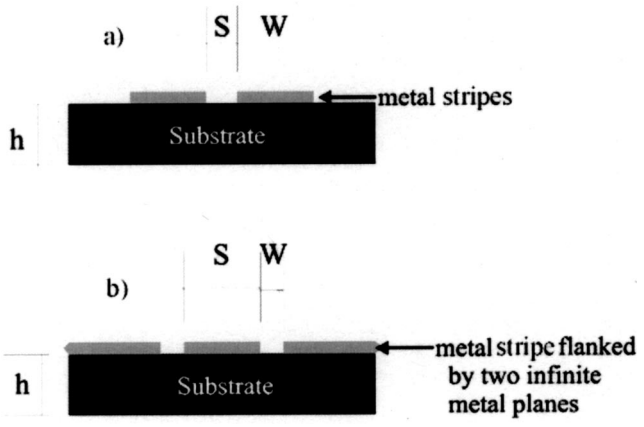

FIG. 8. Sketch of cross sections of a single coplanar stripline (a) and a single coplanar waveguide (b). Coplanar stripline consists of two parallel individual metal stripes. Coplanar waveguide consists of a single metal stripe positioned in between two infinitely large metal areas left and right of it. The two areas have their edges parallel to the stripe.

Here ϵ_e is the effective dielectric constant, that is dependent on the dielectric constant of the substrate and the dimensions of the structures. $K(k)/K(k')$ is only dependent on the dimensions of metal structures.

Using these expressions for the dimensions of sample 1 predicts an impedance of 106 or 64 Ω using formulas (1) and (2), respectively. Table I shows the prediction for sample 2 taking formulas (1) and (2). Due to the nature of the sample used, consisting of an array of parallel lines, none of the two models describes the impedance value accurately. This can be seen in Fig. 8. While coplanar stripline consists of two parallel lines without any other conductor in the vicinity, coplanar waveguide consists of one line with infinitely large planes left and right of it. Therefore the real impedance value should be in the range between the values calculated using formulas (1) and (2).

When the electric field from the tip is perpendicular to the line (TE polarization), a quasi-TEM mode can be excited in the transmission line. This is the dominant mode of this structure and does not have the limitation of a cutoff frequency. It results in an enhanced coupling of energy from a probe into the line structure. When the electric field from the probe is parallel to the lines (TM polarization) no quasi-TEM mode can be excited. In the first case light gets through subwavelength size aperture of the SNOM probe more efficiently and in the second, its greater fraction is reflected back into the probe.

A mode similar to TE_{11} is expected to be excited at the output of the probe. An analytical expression for the impedance[17] is

$$Z_g = \eta \frac{\lambda}{\lambda_g} \tag{3}$$

with $\eta = \sqrt{\mu/\epsilon}$ being the intrinsic impedance and λ_g the guide wavelength. Using formula (3) predicts an impedance value of 83 Ω for a tip with an aperture of 150 nm. Larger aperture sizes result in larger impedance values.

Figure 4(c) shows a maximum intensity at the 400 nm gap size for TE polarization. Taking this result and comparing it to Table I shows that for a gap with 400 nm width the impedance values are 120 or 73 Ω depending on the model used. This suggests that the impedance value of the sample is closer to the one of the coplanar waveguide model which is intuitively clear.

Figure 6 shows the maximum intensity at the 600 nm gap size. Table I suggests an impedance value of 133 or 82 Ω. As impedance is greater at 600 nm separation than at 400 nm, one can expect that the impedance of the SNOM probe in Figs. 6 and 7 is greater than in Figs. 4 and 5. This is consistent with our indication that the probe in Figs. 6 and 7 had a greater aperture. Using the values of Table I we can estimate a 25% larger aperture.

The second possible explanation is based on the excitation of a localized surface plasmon in the gold lines. The surface plasmon can only be detected when scattered at a surface defect, as described before by Hecht *et al.*[15] Surface plasmons on gold are much stronger damped when propagating along the surface compared to plasmon excited in silver. Therefore it is only possible to detect the surface plasmon when the tip is located close to the line edges. The propagation of the surface plasmon is along the direction of the electric field. This approach may explain the increased intensity of the signal in the vicinity of the line edges and its dependence on the light polarization. When the light is TM polarized the surface plasmon will propagate parallel to the line edges and as a result its scattering is hampered. If the light is TE polarized the surface plasmon will propagate perpendicular to the lines and will scatter when reaching the line edge.

The change of the intensity at the sample with the changing gap width could be explained by the generation of a resonance of the surface plasmon in between the edges of the two lines in the gap. This could explain the maximum intensity for a particular gap width.

TABLE I. Impedances for sample 2.

Gap width, S nm	Coplanar stripline impedance, Ω	Coplanar waveguide impedance, Ω
200	100	60
300	111	67
400	120	73
500	127	77
600	133	82

V. CONCLUSIONS

We have presented an experimental study of coupling of polarized light to a mesoscopic metal structure containing Au lines deposited on a Si substrate with varying separation between the lines. We have demonstrated an enhancement of coupling when the polarization direction at the probe is perpendicular to the line edges on the condition that the probe is located in between the lines. On the contrary, the coupling in the case when the probe is located above the metal lines is polarization independent.

The intensity of the enhancement varied depending on the gap width and the tip used reaching the maximum for the

width of 400 or 600 nm depending on the used tip. We gave two possible explanations for this effect, one based on the coupling of light from a circular waveguide into a submicron size optical transmission line and the second one on the excitation of localized surface plasmons.

Using the first approach we could demonstrate that the coupling efficiency depends on the direction of polarization and on the condition when a quasi-TEM mode is launched in the transmission line we observe a substantial enhancement of the coupling efficiency. We have made a prediction for the condition of the maximum coupling efficiency through the approach of impedance matching. By using a sample with various impedance values imaged with probes of different apertures we demonstrated that these predictions hold well, at least semiquantitatively. The values for the optical impedance obtained using the standard microwave formulas must be taken cautiously as in the case of the submicrometer-size structures the skin depth becomes comparable to the size of the transmission line itself. Nonetheless, the concept of optical impedance matching in our view is still valid. In essence it states that the coupling of electromagnetic waves between two structures is maximized when the pattern of electric and magnetic field in one of them matches the same in the other.

The second explanation is based on the excitation of surface plasmons in Au lines. The plasmons propagate in the direction of electric field and scatter at the edges of the metal lines. As a result they can be optically detected.

We believe these results can be of importance in the development of new concepts for high resolution optical imaging by means of SNOM. Samples with variable separation between the lines could be used as test samples to identify the size of the aperture at the tip. It also shows that results depend on tip (polarization, extinction ratio, and aperture size), type of sample (transmission line structures), and the interaction between both. Possibly this could lead to a probe that is not designed as a waveguide but rather as a submicron transmission line, which could provide better extinction ratios. There are recent theoretical and experimental works on the development of nonconventional SNOM probes offering higher light throughput. For example, coaxial SNOM probe was modeled in Ref. 20. In experimental study,[21] massive increase in the throughput was observed for HE11 mode in a new triple-tapered probe.

ACKNOWLEDGMENTS

The authors would like to acknowledge the funding by the EU under the TMR-project NanoSNOM (ERBFMRXCT98-0242), Magnetude Project (G5RD-CT-1999-00005) and by Science Foundation Ireland.

[1] J. R. Krenn, A. Dereux, J. C. Weeber, E. Bourillot, Y. Lacoute, J. P. Goudonnet, G. Schider, W. Gotschy, A. Leitner, F. R. Aussenegg, and C. Girard, Phys. Rev. Lett. **82**, 2590 (1999).
[2] O. Keller, M. Xiao, and S. Bozhevolnyi, Surf. Sci. **280**, 217 (1993).
[3] G. Schider, J. R. Krenn, W. Gotschy, B. Lamprecht, H. Ditlbacher, A. Leitner, and F. R. Aussenegg, J. Appl. Phys. **90**, 3825 (2001).
[4] P. W. Pohl, W. Denk, and M. Lanz, Appl. Phys. Lett. **44**, 651 (1984).
[5] C. Durkan, I. V. Shvets, and J. E. Lodder, Appl. Phys. Lett. **70**, 1323 (1997).
[6] A. Naber, D. Molenda, U. C. Fischer, H. J. Maas, C. Hoppener, N. Lu, and H. Fuchs, Phys. Rev. Lett. **89**, 210801 (2002).
[7] A. Bouhelier, J. Toquant, H. Tamaru, H. J. Guntherodt, D. W. Pohl, and G. Schider, Appl. Phys. Lett. **79**, 683 (2001).
[8] C. Durkan and I. V. Shvets, J. Appl. Phys. **83**, 1171 (1998).
[9] C. Durkan and I. V. Shvets, Ultramicroscopy **61**, 227 (1995).
[10] C. Durkan and I. V. Shvets, J. Appl. Phys. **83**, 1837 (1998).
[11] R. Stockle, C. Fokas, V. Deckert, R. Zenobi, B. Sick, B. Hecht, and U. P. Wild, Appl. Phys. Lett. **75**, 160 (1999).
[12] E. Betzig, P. L. Finn, and J. S. Weiner, Appl. Phys. Lett. **60**, 2484 (1992).
[13] R. Toledo-Crow, P. C. Yang, Y. Chen, and M. Vaez-Iravani, Appl. Phys. Lett. **60**, 2957 (1992).
[14] R. Kantor, M. Lesnak, N. Berdunov, and I. V. Shvets, Appl. Surf. Sci. **145**, 510 (1999).
[15] B. Hecht, H. Bielefeldt, L. Novotny, Y. Inouye, and D. W. Pohl, Phys. Rev. Lett. **77**, 1889 (1996).
[16] A. Gademann, C. Durkan, and I. V. Shvets, J. Phys. D **36**, 2193 (2003).
[17] K. F. Sander, *Microwave Components and Systems* (Addison–Wesley, Reading, MA, 1987).
[18] K. Chang, *Handbook of Microwave and Optical Components* (Wiley, New York, 1989), Vol. 1.
[19] K. Chang, in Ref. 18, Vol. 1, chap. 1.3.
[20] O. Rudow, A. Vollkopf, M. Mueller-Wiegand, G. Georgiev, and E. Oesterschulze, Opt. Commun. **189**, 187 (2001).
[21] T. Yatsui, M. Kourogi, and M. Ohtsu, Appl. Phys. Lett. **73**, 2090 (1998).